

DAMAGE EVOLUTION IN CONCRETE CONSIDERING STOCHASTIC MATERIAL AND BOUNDARY IMPERFECTIONS

M.A. Gutiérrez and R. de Borst
Koiter Institute Delft / Department of Civil Engineering, Delft University
of Technology, Delft, The Netherlands

Abstract

The finite element reliability method is used to study the evolution of localized damage in concrete considering a random damage threshold and random boundary constraints. The difference between deformation measures of selected locations on the solid is used as a state function at different stages of the equilibrium path. The concrete fracture is described by means of a gradient-enhanced damage model. The boundary constraints are imposed through Lagrange multipliers. The influence of the horizontality of the upper loading plate in a direct tension test is presented as an example.

Key words: Gradient-enhanced damage model, Finite element method, Stochastic imperfections, Reliability method, Lagrange multipliers

1 Introduction

Regularization forms an indispensable part in computational localization analysis, since it ensures that the mathematical description remains well-posed after the peak stress has been reached. When damage models are used, this regularization can be achieved by considering non-locality of the strains, either through weighting integrals (Pijaudier-Cabot and

Bažant 1987) or higher-order deformation gradients (Peerlings *et al.* 1996). A proper model of damage evolution is, however, not sufficient to simulate all the phenomena which can take place during failure of concrete. For instance, numerical analyses of tensile tests on double-edge-notched specimens can exhibit a symmetric damage pattern. This is in disagreement with experimental results, in which crack evolution from both notches is seldom observed. In finite element analyses of damage evolution an imperfection is used to trigger localization. Such an imperfection can be introduced by reducing the material strength at some locations or by imposing boundary defects. The onset and evolution of damage is strongly influenced by imperfections, also in the physical reality. It is then meaningful to consider stochastic descriptions of the material as well as boundary imperfections in numerical simulations of concrete failure.

The influence of stochastic material heterogeneities in the evolution of damage has been studied by Carmeliet and de Borst (1995) by means of Monte Carlo simulations and recently by Gutiérrez and de Borst (1998) utilizing the reliability method. This paper presents an extension of the latter approach by considering stochastic variations in the boundary constraints, which are imposed through Lagrange multipliers and can, e.g., consist of prescribed displacements, rigid rotations or elastic supports. The influence of boundary imperfections in the statistics of damage evolution is shown for a tension test on a double-edge-notched specimen.

2 The finite element reliability method

The statistics of the structural response upon a variation of the material properties can be studied by means of the finite element reliability method (Der Kiureghian and Ke 1988). The elaboration of this method for gradient-enhanced material models can be found in Gutiérrez and de Borst (1998). A brief outline is given next.

2.1 Basic strategy

Consider a solid Ω in which the material properties are formalized by a random field. This random field is discretized into a vector of random variables \mathbf{Y} , which, without loss of generality, can be considered to be uncorrelated and standard normally distributed. For a given loading scheme, the equilibrium path $\mathbf{q} = (\mathbf{a}, \lambda)$ can be obtained with a non-linear constrained finite element method for each realization of \mathbf{Y} , where \mathbf{a} represents the nodal displacement and λ is the load multiplier. Since \mathbf{Y} is a random vector, the equilibrium path will be random as well, and a variable transformation can be defined

$$\mathbf{Q} = (\mathbf{A}(\mathbf{Y}), \Lambda(\mathbf{Y})). \quad (1)$$

Uppercase characters represent random variables and lowercase characters represent realizations of these variables. Functions can be defined of the equilibrium path to investigate characteristics of interest, like the peak load, the consumed energy or deformation measures. For a generic characteristic $Z(\mathbf{Q})$, the probability of exceeding a threshold z_0 would formally be expressed by

$$P(Z > z_0) = \int_{z_0}^{\infty} f_Z(z) dz, \quad (2)$$

where f_Z is the probability density function of Z . However, the distribution of \mathbf{Y} is known instead of that of Z . Making use of the variable transformation (1) the probability (2) is recast as

$$P(Z > z_0) = \int_{z(\mathbf{q}(\mathbf{y})) > z_0} \phi(\mathbf{y}) d\mathbf{y}, \quad (3)$$

where ϕ is the uncorrelated standard normal probability density function. The integral (3) is calculated by approximating the surface $z(\mathbf{q}(\mathbf{y})) = z_0$ by a first or second-order surface at the closest point to the origin. When a first-order approximation is used, the probability that Z exceeds z_0 is given by

$$P(Z > z_0) = \Phi(-\beta) \quad (4)$$

where Φ is the one-dimensional standard normal cumulative distribution function and β is the distance from the most central point of $z(\mathbf{q}(\mathbf{y})) = z_0$ to the origin. Accordingly, this point is called β -point.

Finding the β -point is the crucial task in the reliability method. This is achieved by solving an optimization problem,

$$\begin{cases} \text{minimize} & \|\mathbf{y}\| \\ \text{subject to} & z(\mathbf{q}(\mathbf{y})) = z_0 \end{cases} \quad (5)$$

Iterative algorithms are used to search the solution of (5), that need the evaluation of the gradient of $z \circ \mathbf{q}$ with respect to the basic variables \mathbf{y} .

2.2 Computation of the equilibrium path

In a damage model the relation between stress and strain is expressed as

$$\boldsymbol{\sigma} = (1 - \omega(\kappa))\mathbf{D}\boldsymbol{\varepsilon}, \quad (6)$$

where $\boldsymbol{\sigma}$ is the stress tensor, $\boldsymbol{\varepsilon}$ is the strain tensor, \mathbf{D} is the linear elastic operator and ω is the damage loading function which depends on the deformation history κ . When a gradient enhancement is used, the behaviour of the parameter κ is governed by the Kuhn-Tucker conditions

$$\dot{\kappa} \geq 0 \quad \bar{\varepsilon}_{eq} - \kappa \leq 0 \quad \dot{\kappa}(\bar{\varepsilon}_{eq} - \kappa) = 0 \quad (7)$$

and the initial value κ_0 of κ . The average equivalent strain $\bar{\varepsilon}_{eq}$ is obtained from the equation (Peerlings *et al.* 1996)

$$\bar{\varepsilon}_{eq} - \frac{1}{2} l_s^2 \nabla^2 \bar{\varepsilon}_{eq} = \varepsilon_{eq}. \quad (8)$$

The local equivalent strain ε_{eq} is given by any suitable invariant of the strain tensor and l_s is the internal length scale, which quantifies the regularizing effect of the averaging procedure.

The equilibrium path (1) is computed by means of the finite element method. A system results of non-linear equations with an arc-length constraint to monitor the loading,

$$\begin{aligned} \mathbf{r}_a &= \int_{\Omega} \mathbf{B}^T {}^{t+\Delta t} \boldsymbol{\sigma} \, d\Omega - (\Delta\lambda + {}^t\lambda) \mathbf{f}_d = \mathbf{0}; \\ \mathbf{r}_{\Delta\lambda} &= ({}^{t+\Delta t} \mathbf{a} - {}^t \mathbf{a})^T \boldsymbol{\Psi} ({}^{t+\Delta t} \mathbf{a} - {}^t \mathbf{a}) - \Delta l^2 = 0, \end{aligned} \quad (9)$$

where the notation $\gamma(t) = {}^t\gamma$ has been adopted for the sequence of events in a quasi-static process, \mathbf{B} is the strain-nodal displacement matrix, \mathbf{a} is the nodal displacement vector, \mathbf{f}_d represents the nodal design force vector and $\boldsymbol{\Psi}$ is a matrix to select the degrees-of-freedom which contribute to the increment of arc-length Δl . Equation (8) is approximated with the finite element method as well, yielding the system

$$\mathbf{r}_e = \mathbf{K}_{ee} {}^{t+\Delta t} \mathbf{e} - \int_{\Omega} \mathbf{N}^T {}^{t+\Delta t} \boldsymbol{\varepsilon}_{eq} \, d\Omega = \mathbf{0} \quad (10)$$

where \mathbf{N} contains the shape functions and \mathbf{e} is the vector of nodal values of the averaged equivalent strain. Since the equivalent strain and the displacement fields are coupled, equations (9) and (10) are solved simultaneously with the Newton-Raphson method. The Jacobian transformation of the residual \mathbf{r} defined as

$$\mathbf{r} = \begin{pmatrix} \mathbf{r}_a \\ \mathbf{r}_e \\ \mathbf{r}_{\Delta\lambda} \end{pmatrix} \quad (11)$$

can be split in blocks as

$$K = \begin{bmatrix} K_{aa} & K_{ae} & -f_d \\ K_{ea} & K_{ee} & \mathbf{0} \\ ({}^{t+\Delta t}\mathbf{a} - {}^t\mathbf{a})^T \Psi & \mathbf{0} & 0 \end{bmatrix}. \quad (12)$$

Expressions of these blocks can be found in Gutiérrez and de Borst (1998).

2.3 Computation of the gradient of the equilibrium path

In order to find a solution of (5), the gradient of z is needed with respect to the material properties. Since z is a function of \mathbf{q} , this gradient is expressed as

$$\nabla_{\mathbf{y}} z = \nabla_{\mathbf{q}} z \nabla_{\mathbf{y}} \mathbf{q}. \quad (13)$$

The gradient of z with respect to \mathbf{q} can be evaluated explicitly. The gradient of \mathbf{q} , instead, must be computed with aid of the implicit function theorem at an equilibrium point. For a single component of \mathbf{y} we have

$$\frac{\partial \mathbf{r}}{\partial y_i} = \mathbf{0}. \quad (14)$$

The residual \mathbf{r} depends on the variable y_i explicitly, e.g., through the linear elastic operator in equation (6), as well as implicitly, through the nodal variables \mathbf{a} and \mathbf{e} and the loading factor $\Delta\lambda$. Differentiation of equation (14) leads to

$$\underbrace{\left[\nabla_{\mathbf{a}} \mathbf{r}, \nabla_{\mathbf{e}} \mathbf{r}, \frac{\partial \mathbf{r}}{\partial \Delta\lambda} \right]}_{\mathbf{K}} \begin{pmatrix} \frac{\partial {}^{t+\Delta t}\mathbf{a}}{\partial y_i} \\ \frac{\partial {}^{t+\Delta t}\mathbf{e}}{\partial y_i} \\ \frac{\partial \Delta\lambda}{\partial y_i} \end{pmatrix} + \frac{\partial \mathbf{r}}{\partial y_i} \Big|_{(\mathbf{a}, \mathbf{e}, \Delta\lambda)} = \mathbf{0} \quad (15)$$

so that solution of equation (15) yields the required derivatives,

$$\begin{pmatrix} \frac{\partial {}^{t+\Delta t}\mathbf{a}}{\partial y_i} \\ \frac{\partial {}^{t+\Delta t}\mathbf{e}}{\partial y_i} \\ \frac{\partial \Delta\lambda}{\partial y_i} \end{pmatrix} = -\mathbf{K}^{-1} \frac{\partial \mathbf{r}}{\partial y_i} \Big|_{(\mathbf{a}, \mathbf{e}, \Delta\lambda)}. \quad (16)$$

When evaluating the second addend in (15), attention must be paid to the behaviour of the history parameter κ . This is explained in Gutiérrez and de Borst (1998) for the case that \mathbf{y} represents the material parameters and will be elaborated in the next section to evaluate the derivatives of the equilibrium path with respect to boundary constraints.

3 Imposing boundary constraints through Lagrange multipliers

3.1 Equilibrium path

In equation (9) it has tacitly been assumed that some components of \mathbf{f}_d are unknown a priori, to account for the reaction forces induced by the constraints

$$\mathbf{H}\mathbf{a} - \mathbf{c} = \mathbf{0}. \quad (17)$$

Traditionally, these constraints are imposed through transformations of the stiffness matrix \mathbf{K} and the residual \mathbf{r} at each iteration of the Newton-Raphson solution procedure (Crisfield 1991). Such transformations can be troublesome for general forms of \mathbf{H} , e.g., when one degree-of-freedom is affected by more than one constraint. Another possibility is the Lagrange multiplier method (Zienkiewicz and Taylor 1991, Rodríguez-Ferran and Huerta 1998), according to which the reaction forces \mathbf{f}_r are added to the residual \mathbf{r}_a and expressed as

$$\mathbf{f}_r = \mathbf{H}^T \boldsymbol{\mu}, \quad (18)$$

where $\boldsymbol{\mu}$ is a vector of as many Lagrange multipliers as constraints in (17). Defining the residual \mathbf{r}_μ as

$$\mathbf{r}_\mu = \mathbf{H}\mathbf{a} - \mathbf{c}, \quad (19)$$

the system of equations to be solved is

$$\begin{pmatrix} \mathbf{r}_a + \mathbf{H}^T \boldsymbol{\mu} \\ \mathbf{r}_e \\ \Delta\lambda \\ \mathbf{r}_\mu \end{pmatrix} = \mathbf{0}. \quad (20)$$

The Jacobian transformation needed to solve (20) is extended with the matrix \mathbf{H} , rendering the expression

$$\begin{pmatrix} {}^{t+\Delta t}\mathbf{a} \\ {}^{t+\Delta t}\mathbf{e} \\ \Delta\lambda \\ {}^{t+\Delta t}\boldsymbol{\mu} \end{pmatrix}^{(i+1)} = \begin{pmatrix} {}^{t+\Delta t}\mathbf{a} \\ {}^{t+\Delta t}\mathbf{e} \\ \Delta\lambda \\ {}^{t+\Delta t}\boldsymbol{\mu} \end{pmatrix}^{(i)} - \begin{bmatrix} \mathbf{K} & \mathbf{H}^T \\ \mathbf{H} & \mathbf{0} \end{bmatrix}^{-1} \begin{pmatrix} \mathbf{r} \\ \mathbf{r}_\mu \end{pmatrix}^{(i)} \quad (21)$$

for the Newton-Raphson procedure.

Each Lagrange multiplier μ_i in $\boldsymbol{\mu}$ can be interpreted as the generalized force corresponding to the constraint contained in the i -th component of $\mathbf{H}\mathbf{a} - \mathbf{c}$. The independent term \mathbf{c} can in general be considered to be a function of $\boldsymbol{\mu}$ to account for non-rigid connections. For instance, expressions of \mathbf{c} as

$$c_i = k_i^{-1} \mu_i \quad (\text{no sum on } i) \quad (22)$$

would define an elastic connection of the degrees-of-freedom contained in the i -th component of $\mathbf{H}\mathbf{a}$, where k_i is the corresponding stiffness. The Jacobian transformation in (21) then attains the form

$$\begin{bmatrix} \mathbf{K} & \mathbf{H}^T \\ \mathbf{H} & \text{diag}(-k_i^{-1}) \end{bmatrix}. \quad (23)$$

3.2 Gradient of the equilibrium path with respect to the constraints

In the following development it will be assumed that the independent term \mathbf{c} in (17) is composed of constants (thus, not dependent on $\boldsymbol{\mu}$) and represented by the vector \mathbf{Y} of basic random variables. Proceeding in the same fashion as in (14)–(16) we obtain

$$\begin{pmatrix} \frac{\partial {}^{t+\Delta t}\mathbf{a}}{\partial y_i} \\ \frac{\partial {}^{t+\Delta t}\mathbf{e}}{\partial y_i} \\ \frac{\partial \Delta\lambda}{\partial y_i} \\ \frac{\partial {}^{t+\Delta t}\boldsymbol{\mu}}{\partial y_i} \end{pmatrix} = - \begin{bmatrix} \mathbf{K} & \mathbf{H}^T \\ \mathbf{H} & \mathbf{0} \end{bmatrix}^{-1} \frac{\partial}{\partial y_i} \begin{pmatrix} \mathbf{r} \\ \mathbf{r}\boldsymbol{\mu} \end{pmatrix} \Big|_{(a,e,\Delta\lambda,\boldsymbol{\mu})}. \quad (24)$$

Developing terms in the right-hand side of (24) leads to

$$\begin{aligned} \frac{\partial \mathbf{r}\mathbf{a}}{\partial y_i} \Big|_{(a,e,\Delta\lambda,\boldsymbol{\mu})} &= \int_{\Omega} \mathbf{B}^T \left(\frac{\partial {}^{t+\Delta t}\boldsymbol{\omega}}{\partial y_i} \right) \Big|_{(a,e,\Delta\lambda,\boldsymbol{\mu})} \mathbf{D} {}^{t+\Delta t}\boldsymbol{\varepsilon} d\Omega; \\ \frac{\partial \mathbf{r}\mathbf{e}}{\partial y_i} \Big|_{(a,e,\Delta\lambda,\boldsymbol{\mu})} &= \mathbf{0}; \end{aligned} \quad (25)$$

$$\begin{aligned} \frac{\partial \mathbf{r}_{\Delta\lambda}}{\partial y_i} \Big|_{(a,e,\Delta\lambda,\mu)} &= 2({}^{t+\Delta t}\mathbf{a} - {}^t\mathbf{a})\Psi \left(\frac{\partial {}^t\mathbf{a}}{\partial y_i} \right); \\ \frac{\partial \mathbf{r}_\mu}{\partial y_i} \Big|_{(a,e,\Delta\lambda,\mu)} &= -\frac{\partial c}{\partial y_i}. \end{aligned} \quad (25b)$$

The derivative of the damage parameter is formalized as

$$\frac{\partial {}^{t+\Delta t}\omega}{\partial y_i} \Big|_{(a,e,\Delta\lambda,\mu)} = \frac{\partial \omega}{\partial \kappa} \frac{\partial {}^{t+\Delta t}\kappa}{\partial y_i} \Big|_{(a,e,\Delta\lambda,\mu)}. \quad (26)$$

When damage is growing ($\Delta\kappa > 0$) then ${}^{t+\Delta t}\kappa = {}^{t+\Delta t}\bar{\epsilon}_{eq}$. Since $\bar{\epsilon}_{eq} = N\mathbf{e}$, we have

$$\frac{\partial {}^{t+\Delta t}\kappa}{\partial y_i} \Big|_{(a,e,\Delta\lambda,\mu)} = N \frac{\partial {}^{t+\Delta t}\mathbf{e}}{\partial y_i} \Big|_{(a,e,\Delta\lambda,\mu)} = 0. \quad (27)$$

When damage does not grow, then ${}^{t+\Delta t}\kappa = {}^t\kappa$. The derivative of κ attains consequently the value left after at the previous time step, i.e.,

$$\frac{\partial {}^{t+\Delta t}\kappa}{\partial y_i} \Big|_{(a,e,\Delta\lambda,\mu)} = \frac{\partial {}^t\kappa}{\partial y_i}. \quad (28)$$

The derivative of the damage parameter is thus expressed as

$$\frac{\partial {}^{t+\Delta t}\omega}{\partial y_i} \Big|_{(a,e,\Delta\lambda,\mu)} = \begin{cases} 0 & \text{if } \Delta\kappa > 0; \\ \frac{\partial \omega}{\partial \kappa} \frac{\partial {}^t\kappa}{\partial y_i} & \text{otherwise.} \end{cases} \quad (29)$$

4 Example: tension test on a double-edge-notched specimen

The damage evolution in a double-edge-notched plain concrete specimen subjected to an axial, tensile load is presented as an example of the influence of uncertainty in the boundary constraints. The static scheme is depicted in Figure 1. Finite element simulations of this test, in which the loading plates are kept fixed, exhibit a symmetric evolution of damage from both notches if no extra imperfection is imposed. Numerical inaccuracies, however, tend to break this symmetry during the post-peak

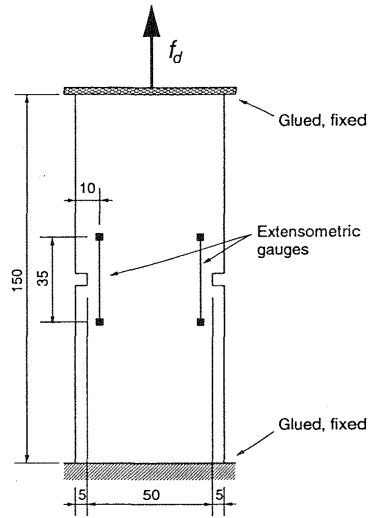


Fig. 1. Schematic representation of a tensile test on a double-edge-notched specimen. Dimensions in millimeters

branch. This is consistent with the unstable behaviour argued by Bažant and Cedolin (1991). On the other hand, experiments show that the deformation pattern is usually asymmetric after the peak load is reached, and evolves to a symmetric pattern during further deformation (Hordijk 1991). The statistics of the relative difference between the extensometric gauges (Figure 1), can be obtained with the finite element reliability method at different stages of the equilibrium path. The damage evolution law is given by

$$\omega(\kappa, \kappa_0) = 1 - \frac{\kappa_0}{\kappa} \left((1 - a) + a \exp(-b(\kappa - \kappa_0)) \right), \quad (30)$$

where the parameters a and b represent the relative reduction of the peak stress as $\kappa \rightarrow \infty$ and the rate at which damage grows respectively. Following Peerlings *et al.* (1998) these parameters are taken $a = 0.96$ and $b = 350$. The equivalent strain ε_{eq} is defined as in de Vree *et al.* (1995),

$$\varepsilon_{eq} = \frac{w - 1}{2w(1 - 2\nu)} I_1 + \frac{1}{2w} \sqrt{\frac{(w - 1)^2}{(1 - 2\nu)^2} I_1^2 + \frac{2w}{(1 + \nu)^2} J_2}, \quad (31)$$

where the strain tensor invariants are given by

$$\begin{aligned} I_1 &= \varepsilon_1 + \varepsilon_2 + \varepsilon_3; \\ J_2 &= (\varepsilon_1 - \varepsilon_2)^2 + (\varepsilon_2 - \varepsilon_3)^2 + (\varepsilon_3 - \varepsilon_1)^2, \end{aligned} \quad (32)$$

and the parameter w controls the sensitivity to compression relative to that in tension. In this study $w = 10$, which means that the compressive strength is ten times larger than the tensile strength. The damage threshold κ_0 of the central zone of the specimen, where the notches trigger localization, is considered to be a normally distributed random field (Figure 5), with mean $E[K_0] = 2.1 \times 10^{-4}$ and coefficient of variation $C_v = 0.1$. A Gaussian correlation function is used,

$$\rho(\mathbf{x}_1, \mathbf{x}_2) = \exp\left(-\frac{|\mathbf{x}_1 - \mathbf{x}_2|^2}{l_c^2}\right), \quad (33)$$

where l_c is the correlation length, which scales the decay of the correlation function as the distance between \mathbf{x}_1 and \mathbf{x}_2 increases. In this study $l_c = 10$ mm. The other material parameters have been taken $E = 18\,000$ MPa, $\nu = 0.2$ and $l_s = \sqrt{2}$ mm. A design load of 7 000 N has been considered.

The random field of the damage threshold is discretized with the midpoint method (Li and Der Kiureghian 1993) and the specimen, that has a thickness of 50 mm, is discretized into eight-noded plane-stress finite elements with a 2×2 Gauss-Legendre integration quadrature. While the nodes along the bottom edge are kept fixed, linear constraint equations are used along the top edge to simulate a fixed plate. The difference between the vertical displacement of the left and right uppermost corners is tied as well and considered as a centered, normally distributed random variable. Different values will be considered for the standard deviation σ_p of this variable in order to simulate defects in the horizontality of the loading plate. Although a realistic analysis should also consider the bending stiffness of this plate, we shall assume that it is rigid so as to study the consequences of an orientation defect exclusively. The servo-control by the extensometric gauges is simulated with a selective arc-length procedure.

Defining δ_l and δ_r as the extension of the left gauge and the right gauge respectively, the state function Z is defined as

$$Z(\Delta_l, \Delta_r) = \frac{\Delta_r - \Delta_l}{(\Delta_r + \Delta_l)/2} \quad (34)$$

in order to study the relative difference of extension between both gauges. Different points of the cumulative distribution function of Z can be obtained by running the reliability algorithm for different values of z_0 . Due to the symmetry of the problem, it is meaningful to study the probability that the absolute value of the difference (34) exceeds a threshold. A first-order approximation of this probability is readily expressed as

$$P(|Z| > z_0) = P(Z < -z_0) + P(Z > z_0) \approx 2\Phi(-\beta). \quad (35)$$

Table 1. Results for $\sigma_p = 0$ mm

$(\delta_l + \delta_r)/2$	0.008 mm		0.014 mm	
z_0	0.3	0.15	0.3	0.15
β	0.88	0.42	1.46	0.72
$P(Z > z_0)$	0.378	0.674	0.144	0.474

Table 2. Results for $\sigma_p = 0.0005$ mm

$(\delta_l + \delta_r)/2$	0.008 mm		0.014 mm	
z_0	0.3	0.15	0.3	0.15
β	0.86	0.41	1.42	0.70
$P(Z > z_0)$	0.390	0.682	0.156	0.484

Table 3. Results for $\sigma_p = 0.005$ mm

$(\delta_l + \delta_r)/2$	0.008 mm		0.014 mm	
z_0	0.3	0.15	0.3	0.15
β	0.35	0.17	0.47	0.23
$P(Z > z_0)$	0.726	0.865	0.638	0.818

The statistics of the relative difference of gauge extensions has been studied at two different stages of the post-peak equilibrium path, namely for $(\delta_l + \delta_r)/2 = 0.008$ mm and $(\delta_l + \delta_r)/2 = 0.014$ mm, which approximately correspond to 100% and 75% of the peak load respectively. In the first simulation it has been assumed that the loading plate is perfectly horizontal, i.e., $\sigma_p = 0$ mm. Uncertainty is thus only found in the damage threshold field. The results, which are shown in Table 1, show that the probability of keeping a given degree of asymmetry (quantified by z_0) decreases as the average deformation progresses. A second simulation has been carried out for $\sigma_p = 0.0005$ mm. Table 2 shows that the results do not essentially differ from those obtained for $\sigma_p = 0$ mm. The probabilities of exceeding z_0 are slightly larger in this case. When $\sigma_p = 0.005$ mm, instead, a dramatical grow of these probabilities is observed (Table 3). This results show that small defects in the orientation of the loading plate can be of capital importance for the asymmetry in the evolution of the damage pattern during failure.

5 Conclusions

It is meaningful to consider uncertain boundary constraints in probabilistic

analysis of fracture processes of concrete, since the statistics of the damage evolution can depend significantly on the boundary defects. Evaluation of this dependence is possible with the finite element reliability method. For this purpose, stochastic boundary conditions can efficiently be imposed through Lagrange multipliers.

6 References

- Bažant, Z.P. and Cedolin, L. (1991), **Stability of structures**, Oxford University Press, New York
- Carmeliet, J. and Borst, R. de (1995), Stochastic approaches for damage evolution in standard and non-standard continua, **Int. J. Solids Structures**, 32, 1149–1160
- Crisfield, M.A. (1991), **Non-linear finite element analysis of solids and structures**, Wiley, Chichester
- Der Kiureghian, A. and Ke, J.B. (1988), The stochastic finite element method in structural reliability, **Probabilistic eng. mech.**, 3, 83–91
- Gutiérrez, M.A. and de Borst, R. de (1998), Computational analysis of the influence of stochastic heterogeneities in concrete fracture using a gradient-enhanced damage model, **Computational modelling of concrete structures** (Eds. R. de Borst *et al.*), Balkema, Rotterdam
- Hordijk, D.A. (1991), **Local approach to fatigue of concrete**, Dissertation, Delft University of Technology
- Li, C.C. and Der Kiureghian, A. (1993), Optimal discretization of random fields, **J. Eng. Mech.**, 119, 1136–1154
- Peerlings, R.H.J., Borst, R. de, Brekelmans, W.A.M. and Vree, J.H.P. de (1996), Gradient-enhanced damage for quasi-brittle materials, **Int. J. Numer. Meth. Engrg.**, 39, 3391–3403
- Peerlings, R.H.J., Borst, R. de, Brekelmans, W.A.M. and Geers, M.G.D. (1998), Gradient-enhanced damage modelling of concrete fracture, **Mechanics of cohesive-frictional materials**, in press
- Pijaudier-Cabot, G. and Bažant, Z.P. (1987), Nonlocal damage theory, **J. Eng. Mech.**, 113, 1512–1533
- Rodríguez-Ferran, A. and Huerta, A. (1998), Adapting Broyden method to handle linear constraints imposed via Lagrange multipliers, **Int. J. Numer. Methods Engrg.**, accepted for publication
- Vree, J.H.P. de, Brekelmans, W.A.M. and Gils, M.A.J. van (1995), Comparison of nonlocal approaches in continuum damage mechanics, **Comput. Struct.**, 55, 581–588
- Zienkiewicz, O.C. and Taylor, R.L. (1991), **The finite element method**, 1 & 2, McGraw Hill, London